

## Article

# Effects of Saline Solutions on Paper-Based Cultural Heritage: Non-Invasive Techniques for Studying Flooded Ancient Books

Tullia Carla David <sup>1</sup>, Francesca Assunta Pisu <sup>1</sup>, Stefania Porcu <sup>1,\*</sup>, Carlo Maria Carbonaro <sup>1</sup>, Jarmila Kodric <sup>2</sup> and Daniele Chiriu <sup>1,\*</sup>

<sup>1</sup> Department of Physics, University of Cagliari—Cittadella Universitaria, 09042 Monserrato, Italy; davidtulliacarla@gmail.com (T.C.D.); fpisu@dsf.unica.it (F.A.P.); cm.carbonaro@dsf.unica.it (C.M.C.)

<sup>2</sup> Alma Mater Europaea Ecm, 2000 Ljubljana, Slovenia; jarmila.kodric@gmail.com

\* Correspondence: stefania.porcu@dsf.unica.it (S.P.); daniele.chiriu@dsf.unica.it (D.C.)

**Abstract:** Archival materials are increasingly vulnerable to damage from chemical, physical, biological, and environmental factors, including climate change-related extreme weather events such as torrential rains and flash floods. These conditions pose significant risks to paper-based cultural heritage, leading to degradation from both water and salt exposure. This study investigates the effects of direct immersion in saline solutions on different types of paper, simulating the impact of flooding events. We focused on how varying levels of salinity affect the crystalline structure of paper, which is crucial for understanding its degradation. This study employed non-invasive, portable optical techniques such as luminescence, reflectivity, and Raman spectroscopy to monitor the changes in the paper structure. Our results showed that salt exposure leads to significant alterations in the paper's crystalline composition. The study concludes that washing treatments are essential for mitigating further degradation, highlighting the importance of timely intervention in preserving cultural heritage. The non-destructive nature of the methods used also demonstrates their potential for in situ applications in cultural heritage conservation.

**Keywords:** preservation; chemical; physical; and biological phenomena; preventive conservation-restoration measures; hydrogeological phenomena; optical techniques; portable measurements; cultural heritage



Academic Editors: Nicola Masini, Paola Fermo and Giuseppe Politi

Received: 2 December 2024

Revised: 6 January 2025

Accepted: 17 January 2025

Published: 24 January 2025

**Citation:** David, T.C.; Pisu, F.A.; Porcu, S.; Carbonaro, C.M.; Kodric, J.; Chiriu, D. Effects of Saline Solutions on Paper-Based Cultural Heritage: Non-Invasive Techniques for Studying Flooded Ancient Books. *Heritage* **2025**, *8*, 40. <https://doi.org/10.3390/heritage8020040>

**Copyright:** © 2025 by the authors. Licensee MDPI, Basel, Switzerland. This article is an open access article distributed under the terms and conditions of the Creative Commons Attribution (CC BY) license (<https://creativecommons.org/licenses/by/4.0/>).

## 1. Introduction

In today's world, libraries and archives worldwide are struggling with a range of serious problems. Many of their documents and assets are fragile, making even their basic use risky. This situation affects both public and private collections and politicians because cultural items, like old papers, pictures, and sculptures, are not just old; they are like time machines that help us to understand where we came from and to feel in close connection to our ancestors. The vulnerability of these items stems from various factors, including exposure to chemicals, physical harm, and infestation by pests [1–3]. However, the issue extends further than these immediate threats. There is often a lack of prevention measures to circumvent these problems, such as inadequate protection systems and restoration protocols in case of damage due to unexpected disasters. Furthermore, maintaining ideal environmental conditions for preservation remains a persistent challenge.

A large part of cultural heritage archives are represented by paper supports. Understanding the properties of paper and their relation to historical production processes is crucial for both appreciating human communication's evolution and developing effective conservation strategies. Ancient papermaking techniques, such as the use of textile

waste and manual craftsmanship, illustrate the track of civilization and provide essential knowledge for preservation efforts [4–8].

Furthermore, knowing the materials and processes used over centuries to create paper enables us to develop effective strategies for its conservation and protection [9]. This is particularly vital today, as many paper resources and historical documents are fragile and require targeted interventions to prevent deterioration.

Table 1 summarizes key developments in papermaking techniques and materials across different periods, highlighting their evolution and significance.

**Table 1.** Key development in papermaking techniques and materials across different periods.

Period	Material Used	Key Techniques	References
Mid-1200s	Hemp, flax, cotton rags	Introduction of animal gelatin sizing	[10]
Early 19th century	Rag pulp, wood pulp	Refining, sizing with alum, rosin	[11,12]
Mid-1900s	Synthetic fibers, wood pulp	Mechanized refining and additives	[13,14]

Traditionally, handmade paper was crafted predominantly from hemp, flax, and cotton rags.

Rags, initially collected by private vendors and later regulated by the state, served as the primary raw material. These rags were meticulously sorted based on color and quality. The transition from discarded textiles to refined paper involved multiple steps: rinsing, fermenting with lime, manual or mechanical refining, and sizing.

The selection of rags was meticulous, favoring those composed of plant fibers. They were further categorized into white and colored, as well as fine, medium, and coarse, depending on the desired paper quality. Despite their origins as discarded garments, often colored, rag fibers were valued for their quality due to the natural refining process from frequent use and washing [15].

Notable advancements, such as the use of animal gelatin for sizing in Fabriano during the 1200s, enhanced paper's durability and strength.

Until the mid-1900s, rags remained a primary material for paper production. However, the rise of synthetic fibers complicated the sorting and collection of plant-based rags, making it costly and challenging [13]. The transition from rags to paper involved a multi-step process, beginning with rinsing and fermenting the fibers with lime to soften them for easier handling. Refining followed, where fibers were separated and shortened to prevent tangling during production. Initially done manually, refining later shifted to mechanical methods powered by water mills [16].

The pulp, once refined, was collected and placed on a frame for drainage and paper formation. After drying, sizing ensured the paper's strength and smoothness. This process, called "calendering", evolved from manual methods to mechanized ones using wooden and metal cylinders.

By the early 19th century, advancements in chemistry enabled the extraction of cellulose from wood and other plant materials, introducing wood pulp as a viable alternative to rags. The shift to wood fibers significantly changed paper's properties, including its strength, texture, and durability. Wood pulp paper, while more economical, often contained impurities that made it more susceptible to degradation over time compared to rag-based paper. Despite this drawback, its prevalent adoption marked a turning point in papermaking [11].

Additives like binders (e.g., starch, gelatin) and mineral fillers (e.g., kaolin, talc, dolomite, barium sulfate and satin white) further improved paper's properties, such as smoothness and resistance to ink spread. Techniques like "bluing" were later developed to

counteract discoloration of fibrous materials, ensuring the longevity and aesthetic appeal of paper products and maintain paper's aesthetic appeal [6,14,17–19].

The preservation of paper requires a thorough assessment of its degradation state, which involves analyzing cellulose's crystallinity and polymerization degree [20–22].

Paper degradation is influenced by a variety of factors, including environmental conditions, chemical reactions, and biological agents [23], with saltwater exposure posing a significant risk due to its potential to accelerate fiber weakening and structural damage [24–26].

This study investigates the degradation of various types of paper, each with different compositions and properties, following immersion in water with different salinity levels and successive natural or forced drying at 50 degrees. The choice of salt water as degradation agent is related to the provenience of some paper samples belonging to private collection from Venice (Italy) and the recurring problem of sea flooding in that city.

The research begins with an optical characterization of the paper samples, followed by a comprehensive analysis using Raman spectroscopy to evaluate the degree of polymerization of the cellulose and the crystallinity index after undergoing different treatments.

Additionally, a colorimetric and morphological analysis is conducted to provide a detailed understanding of the degradation processes.

## 2. Materials and Methods

### 2.1. Samples

The samples analyzed in this study involved five distinct types of paper:

- Sample Ref: Whatman 1 paper is produced from pure cellulose pulp.
- Sample A: Fabriano paper, produced in 1983, consists mainly of cellulose with a low percentage of lignin. Bleaching additives were employed during its manufacturing process. It has a weight of 70 g/m<sup>2</sup> and exhibits a thin and compact appearance.
- Sample B: “cinquecentine's” paper, made of cellulose pulp but with a lower degree of purity of whatman 1, and containing animal gelatin (private collection and CA Archive).
- Sample C: Bluing paper, originating from 1828, composed of linen and cotton fibers and manufactured using rags, animal gelatin, and mineral fillers. It displays a bluish-yellow color and possesses a thick, rough, and rigid texture (private collection).
- Sample D: Printing paper from the library collection, dated 1901 and industrially manufactured. It contains a significant amount of lignin, giving it the characteristic yellowish color associated to papers with high content of this molecule (private collection).

### 2.2. Treatments

The samples underwent various treatments with water solutions and drying procedures. The solutions were prepared at different salinity levels to mimic treatments with brackish water (1%), standard marine saltwater (3%), and brine (5%). Specifically, for seawater (SeaW) solutions, a standard composition was employed (Table 2) [27].

Only sodium chloride (NaCl) was used for home-made saltwater (SW) solutions, with concentrations of 1%, 3% and 5%. Additionally, a treatment with distilled water (DW), corresponding to 0% salt concentration, was conducted for each sample.

The samples, measuring approximately 3 cm × 1.5 cm, were immersed in 20 mL of room-temperature solutions to preserve thermolabile properties.

Following immersion, two drying methods were employed: one at room temperature (RT) of 25 °C (slow drying) and another in a controlled temperature environment (T) of 50 °C (see Figure 1 and Table S1).

**Table 2.** Standard composition of seawater.

Salt (mg)	Compound
20,747	NaCl
9474	MgCl <sub>2</sub> · 6H <sub>2</sub> O
1326	CaCl <sub>2</sub> · 2H <sub>2</sub> O
3505	Na <sub>2</sub> SO <sub>4</sub>
597	KCl
171	NaHCO <sub>3</sub>
85	KBr
34	Na <sub>2</sub> B <sub>4</sub> O <sub>7</sub> · 10H <sub>2</sub> O
12	SrCl <sub>2</sub>
3	NaF
1	LiCl
0.1042	Others

**Figure 1.** Studied samples.

The pH of the solutions was measured using an Adwa AD11 calibrated pH meter prior to the immersion of the samples and monitored throughout the experiments. The pH of the solutions was between 5.5 and 5.8, and these values remained unchanged throughout the experimental process.

All the measurements were carried out on three replicas in different points for each sample.

### 2.3. Study of the Degradation Process

Several reference studies demonstrate that cellulose degradation follows a first-order kinetic [28,29] with a rate equation in the form:

$$\frac{dA}{dt} = k$$

In the case of a linear polymer subject to a random degradation, the general term  $A$  is replaced by the total number of unbroken intermonomer bonds remaining (number of chains times the number of monomer units in the chain minus one). In a kinetic model proposed in a previous work [29], we assumed that the length of the polymer chain at a fixed time, that is the number of inter-monomer bonds at that time, is proportional to the  $I_{1093}/I_{1376}$  ratio between the intensity of two Raman bands at 1093 and 1376  $\text{cm}^{-1}$  by following the equation:

$$\left(\frac{I_{1093}}{I_{1376}}\right)_t \propto l_t$$

From the previous relation, at fixed time, one can study the relative variation of the number of intermonomer bonds  $l$  as a function of the interaction between cellulose and intentional environmental agents, such as light, temperature or water immersion. The parametrization of this relative variation can be implemented by calculating the ratio  $R_{C-O-C}$  between the number of intermonomer bonds of a treated sample and the same quantity determined in an untreated sample:

$$R_{C-O-C} = \frac{\left(\frac{I_{1093}}{I_{1376}}\right)_{treated}}{\left(\frac{I_{1093}}{I_{1376}}\right)_{untreated}} = \frac{l_{treated}}{l_{untreated}}$$

The ratio  $R_{C-O-C}$  can be defined as the relative polymerization grade. Analogously, the relative crystallization index of cellulose is determined studying the ratio  $I_{900}/I_{1376}$  between the intensity of two Raman bands at 900 and 1376  $\text{cm}^{-1}$  through the following relation:

$$CI = \frac{\left(\frac{I_{900}}{I_{1376}}\right)_{treated}}{\left(\frac{I_{900}}{I_{1376}}\right)_{untreated}}$$

### 2.4. Reflectance Measurements

UV-Vis-NIR solid-state reflectance spectra were collected (applying baseline corrections) by a Jasco V-750 (JASCO Europe S.R.L., Cremella (LC), Italy) spectrophotometer with a spectral bandwidth of 2 nm in the 200–900 nm range. The measurements were taken using a  $\text{BaSO}_4$  plate as a reference.

### 2.5. Colorimetric Analysis

The results obtained from the reflectance measurements were related to the D65 illuminant and the CIE Lab standard colorimetric observer. The CIE coordinates were obtained by using the ColorConvert v7.77 software. The color change was characterized according to the change in brightness  $\Delta L$ , red–green difference  $\Delta a$ , yellow–blue difference  $\Delta b$ , and total calculation of color difference  $\Delta E$  using the following formula:

$$\Delta E = \sqrt{(\Delta L)^2 + (\Delta a)^2 + (\Delta b)^2}$$

### 2.6. Photoluminescence Measurements

Photoluminescence of samples was determined using a spectrofluorometer, a Jasco FP-8050, with a 450 W Xenon lamp as the excitation source. The spectra were collected with an excitation of 400 nm and an emission range of 500–800 nm with a 5 nm spectral bandwidth.

### 2.7. Raman Measurements

Micro-Raman spectra were obtained from solid molecules through the Near infrared micro Raman B&W-TEK (Newark—USA) i-Raman Ex integrated system in back scattering geometry with the 1064 nm line of an Nd:YAG laser. The experimental setup, equipped with the Video Micro Sampling System BAC151B and a 20× Olympus objective, guarantees a spectral resolution of 8 cm<sup>-1</sup>.

### 2.8. SEM Imaging and EDS

SEM images were gathered by a scanning electron microscope ESEM: FEI Quanta 200 (FEI Company, Hillsboro, OH, USA) under low-vacuum conditions. EDS semiquantitative analyses were obtained with the help of Thermo Scientific EDS UltraDry INTX-10P-A (Thermo Fisher Scientific, Waltham, MA, USA) system equipped with Pathfinder. Each point of analysis was collected with an acceleration voltage of 20 kV and live time of 30 s.

## 3. Results and Discussion

The degradation process of the paper was studied using a multi technique approach.

Firstly, the attention was devoted to the study of paper luminescence. As reference standard, we choose the Whatman 1 paper because of its composition (pure cellulose) that conveys to the reference the larger resilience to the investigated treatments as compared to the other samples.

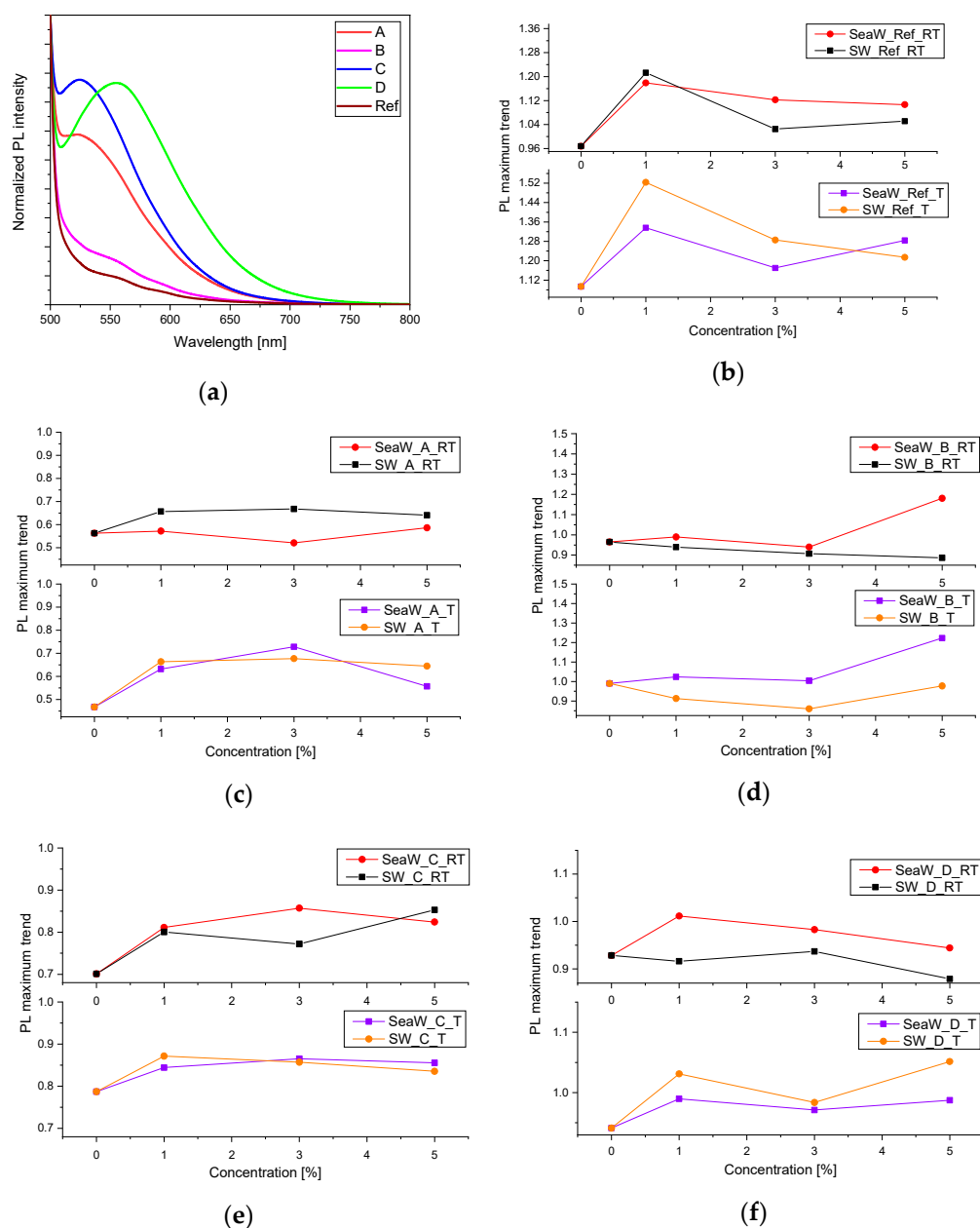
For a preliminary study of the reference standard, a photoluminescence (PL) spectrum was acquired with an excitation wavelength of 400 nm, revealing the presence of a weak band at 546 nm (known from literature to be associated with cellulose and paper degradation [17]), which was further investigated.

Figure 2a displays all the PL curves acquired in the 500–800 nm range for the various samples, underlining the differences among them, possibly associated to the different compositions. The PL spectra were normalized to the standard emission of cellulose paper at 460 nm observed in the whole set of samples [30].

In the reference [31] sample, we observed the presence of two bands with low intensity at about 554 and 580 nm. The same bands were also detected in sample B, whilst the other samples show a single large contribution, with the emission peaked at 524 nm for samples A and C and at 554 for sample D. The increase in the PL intensity might be associated with the presence of additives in the paper fabrication [31].

The first approach on understanding the degradation process involves the analysis of the variations in the luminescence for all the studied samples treated with both seawater and saltwater solutions and dried both at room temperature of 25 °C (RT) and at 50 °C (T). (Figures 2b–f and S1 in Supporting Information).

From the study of the reference (Figure 2b), it is possible to observe an increase in the peak intensity at 546 nm for the sample treated with 1% concentration saltwater and dried at 50 °C (orange plot), while a decrease is observed as the concentration increases. The same trend, even though less pronounced, is observed in the plot of the sample treated with saltwater and dried at room temperature.



**Figure 2.** (a) Photoluminescence (PL) spectra of all samples acquired with an excitation wavelength of 400 nm. (b–f) Trend of the luminescence for all the studied samples treated with both seawater and saltwater solutions and dried at both room temperature of 25 °C (RT) and at 50 °C (T).

When comparing the graphs considering only the drying temperature, the samples dried at 50 °C show greater variations compared to the untreated sample. However, the trend of the luminescence maximum of the samples immersed in seawater remains almost constant and seems not to be influenced by the salt concentration level of the solution.

For sample A (Figure 2c), emerged that following the various treatments, the band shows a decrease in intensity and the maximum intensity variation occurs when the sample is treated with distilled water and then dried at 50 °C. No significant variations are observed as a function of salt concentration.

In the trend representative of sample B (Figure 2d), when treated with both seawater and saltwater solutions, we observed an increase in intensity of the band centered at 546 nm with an increase in the concentration of the two solutions whether the sample is dried at room temperature or at T = 50 °C.

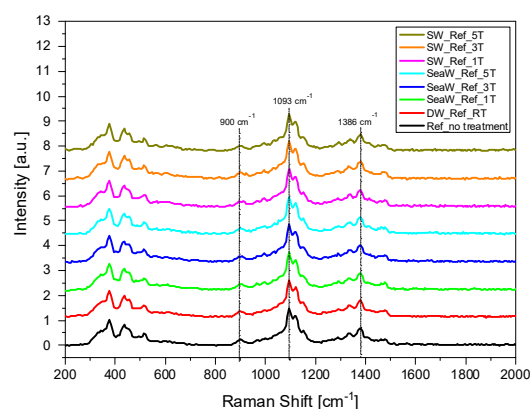
Independence from the drying process is also evident in the samples that were immersed in distilled water. Furthermore, it is worth noting that the variation is very small compared to the intensity value that the maximum assumes in the untreated sample B.

Figure 2e shows the trends of the maximum intensity of the 524 nm band in sample C. The samples treated with distilled water show the greatest variation. We notice that for samples treated with saltwater and dried at room temperature, there is a slight increase in the maximum intensity as a function of concentration, while in all the other cases, this trend remains constant.

Finally, from the analysis of the luminescence of sample D (Figure 2f), a decreasing trend is evident as a function of concentration for the samples dried at room temperature. In particular, the 5% saltwater solution appears to decrease the intensity of the peak more significantly compared to what happens for the sample immersed in distilled water. In the case of drying at 50 °C, the trend is constant for the seawater solution, while a positive slope is observed for the samples treated with saltwater.

To comprehensively explore the effects of different treatments, we performed an extensive analysis regarding the polymerization degree and the crystallinity index of the cellulose by Raman measurements.

Figure 3 illustrates the Raman spectra acquired for both untreated and treated reference sample, including all utilized concentrations. All the samples showed the same main characteristics in the Raman spectra with, in addition, a peak at 1600 cm<sup>-1</sup> associated with the presence of lignin in the sample.



**Figure 3.** Raman spectra acquired for both untreated and treated reference sample, including all utilized concentrations.

The observed peaks in the scattering pattern correspond to the features of cellulose. Peak assignments, extracted from literature references [30], helped in the interpretation of spectral data and are detailed in Table 3.

Using Raman spectroscopy, it was possible to study both the trend of cellulose polymerization degree (RC-O-C) and its crystallinity index (CI), studying the ratio between the intensity of the band at 1093 cm<sup>-1</sup> and the band at 1376 cm<sup>-1</sup>, and the ratio between the intensity of the bands at 900 and 1376 cm<sup>-1</sup> (see S2 in Supporting Information).

The results of the polymerization degree (RC-O-C) are summarized in Figure 4. A negative variation corresponds to a break of cellulose polymers and shortening of chains, which occurs in the samples treated with distilled water, as the drying process affects the length of cellulose chains. In particular, the drying process at room temperature seems to elongate them, which could be due to the fibers, being hydrated and undergoing slow drying, having the necessary time to create new bonds with other glucose units.

**Table 3.** Raman peak assignments.

Raman Shift (cm <sup>-1</sup> )	Assignments
376	Twisting and bending C-C-C of the pyranic ring
437–504	Bending C-C-O
900	Crystallinity of cellulose
1093	Stretching C-O-C β-glycosidic
1316	Bending C-O-H, H-C-C
1335	Bending C-H
1376	Bending C-H
1425	Bending H-C-H, O-C-H

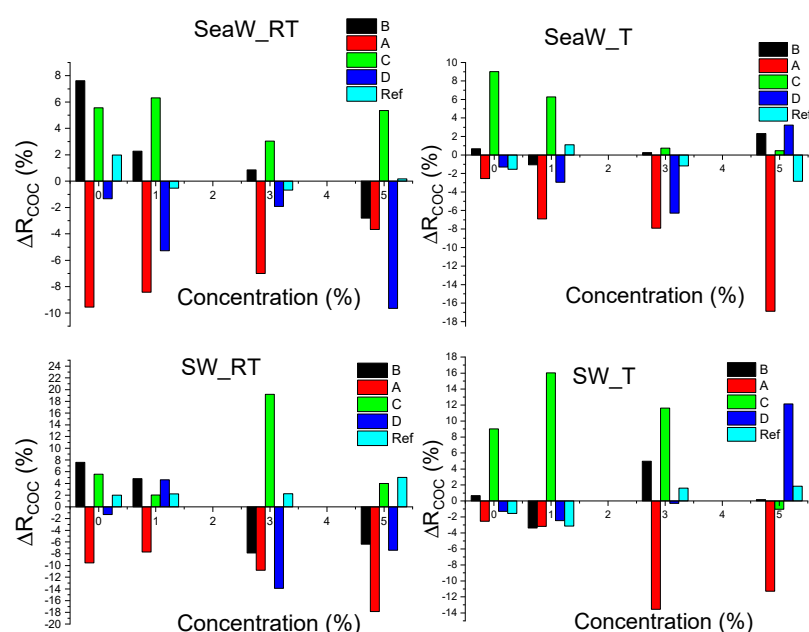


**Figure 4.** The variation in the polymerization degree after treating the samples with seawater and salt water at different concentrations and after drying them at room temperature or 50 degrees. A, B, C, D, E and Ref correspond to Fabriano paper, Cinquecentine’s paper, bluing paper, printing paper and paper from library collection and Whatman 1, respectively.

This phenomenon does not happen in the case of fast drying, where the fiber, dehydrating quickly, does not have enough time to relax and create new bonds; on the contrary, the temperature and mechanical stresses to which the chain is subjected could even break the bonds, thereby shortening the chains.

In the case of treatment with seawater solution, drying at 50 °C might mitigate this process because the presence of salts seems to somehow protect and stabilize the fibers despite rapid dehydration. However, an increase in salt concentration shows a decrease in this protective effect.

In the case of saltwater, an opposite trend is observed. Comparing the graphs where drying was performed at room temperature, a decrease in  $R_{C-O-C}$  is observed when the samples were immersed in seawater solution. However, both solutions cause the degree of polymerization to increase with increasing concentration. This behavior is associated with the presence of the lignin that plays a crucial role in favoring the depolymerization process.

Regarding the crystallinity index of cellulose shown in Figure 5, a negative variation corresponds to a lower crystallinity of cellulose. All graphs show a constant trend with a

decrease in CI as a function of salt concentration irrespective of the treatment. The exception is represented by the C samples where a general increase in CI is observed with increasing concentration but at the largest one.

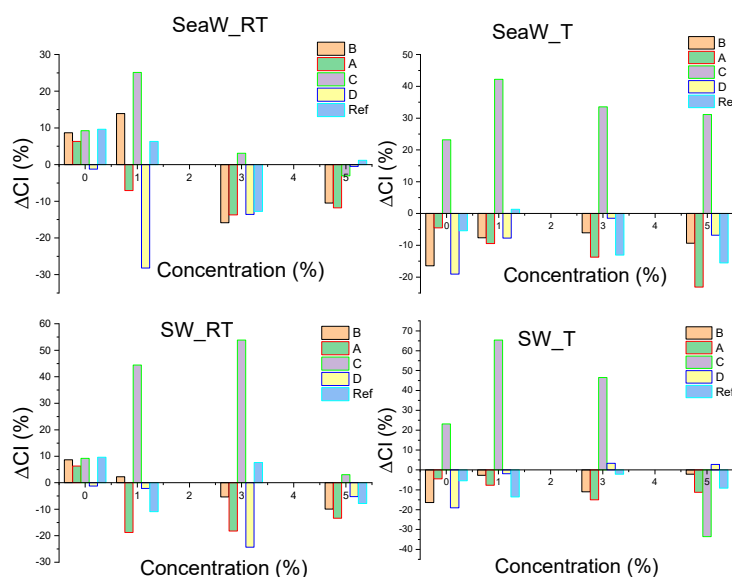


**Figure 5.** Variation in the crystallinity index after treating the samples with seawater and salt water at different concentrations and after drying them at room temperature or 50 degrees. A, B, C, D, E and Ref correspond to Fabriano paper, Cinquecentine’s paper, bluing paper, printing paper and paper from library collection and Whatman 1, respectively.

The increasing trend in the crystallinity index (CI) of sample C with higher salt concentrations may be explained by the interaction between the salt ions and the amorphous regions of the cellulose fibers. Salts may preferentially interact with or disrupt these less-ordered regions, potentially facilitating the reorganization or aggregation of cellulose chains into more ordered, crystalline structures.

Additionally, the higher ionic strength in solutions with greater salt concentrations could reduce the electrostatic repulsion between cellulose chains, promoting closer packing and an apparent increase in crystallinity.

We observed also that forced drying (50 degrees) and increased salt concentration stress the fibers, causing them to reassemble in a disordered manner, leading to a decrease in crystallinity index and polymerization degree as well as discussed above. In this case, it is worth noting that the role of the surface additives (usually called the “charge”) is to preserve crystallinity and avoid disorder.

During the different treatments, we observed a change in the color of the sample observable in the reflectance spectra (see S3 in Supporting Information); we conducted a more in-depth study to investigate variations in colorimetric coordinates. From the reflectance spectra, indeed, it is possible to highlight a substantial variation in the UV region, associated with phenomena related to the structure modification.

All coordinates show a variation, although small, compared to the initial values. However, with the same saline treatment and drying, it is observed that the calculated differences for coordinate ‘a’ remain constant, while the coordinate showing the greatest variation among all is the brightness coordinate ‘L’ (see S4 in Supporting Information).

Analyzing sample A, the highest overall color variation ( $\Delta E$ ) was found in the sample treated with a 1% concentration seawater solution. This finding suggests that the presence of saltwater, even at relatively low concentrations, significantly affects the color properties of the samples. Notably, the sample dried at 50 °C, exhibiting a pronounced decrease in

brightness accompanied by a noticeable shift towards blue shades. This shift could be attributed to various factors, including chemical reactions induced by the drying process and the interaction between the saline solution and the sample material.

Furthermore, in sample B, it is highlighted that for all conducted treatments, there is a discernible shift in color towards yellow shades ('b' coordinate). Interestingly, the greatest overall color variation is observed for the samples treated with distilled water and dried at 25 °C, as well as those immersed in saltwater and subjected to drying at 50 °C. These findings suggest that both the type of treatment solution and the drying temperature play crucial roles in determining the extent of color variation.

In sample C, all treatments contribute to a chromatic shift towards blue. This caused an unexpected trend towards blue shades in the samples.

Finally, for sample D, the colorimetric coordinates show that the greatest overall color variation is evident for the sample treated with 1% concentration seawater and dried at 50 °C. This result supports the earlier findings regarding the significant impact of saltwater treatment and high drying temperatures on color properties.

Table 4 summarizes the results relating to the total color variation for all the studied samples, both treated and untreated, across different concentrations. It highlights that the greatest variations in terms of colorimetric coordinates were observed for the azure paper (sample C), specifically for the sample treated with 1% concentration seawater and dried at 50 °C. One plausible explanation could be the removal of additives, such as bleaching agents, during the treatment process. As these additives are washed away, the intrinsic blue dye within the samples may become more apparent, leading to the observed shift towards blue shades.

**Table 4.** Total color variation for all the studied samples, both treated and untreated, across different concentrations.

Sample	deltaE															
	SeaW RT				SW RT				SeaW T				SW T			
	0%	1%	3%	5%	0%	1%	3%	5%	0%	1%	3%	5%	0%	1%	3%	5%
Ref	0.18	0.52	0.33	1.18	0.18	0.25	0.14	0.37	0.33	0.20	0.86	0.67	0.33	0.09	0.20	0.69
A	0.55	1.01	0.82	0.58	0.55	0.70	0.95	0.05	0.84	1.60	0.21	1.01	0.84	0.44	0.36	0.72
B	2.24	1.28	1.25	1.54	2.24	1.34	0.99	1.05	0.88	1.36	1.34	1.79	0.88	1.58	0.29	2.03
C	5.93	6.57	6.66	5.95	5.93	5.92	5.47	6.82	5.90	6.94	6.60	6.74	5.90	6.49	5.65	6.16
D	1.49	3.33	1.39	1.54	1.49	1.97	1.33	0.69	2.65	4.18	1.22	3.19	2.65	2.68	0.91	1.22

SEM-EDX measurements provide crucial insights into the structural transformations induced by the treatments on paper substrates.

In Figure 6, SEM images show distinct morphological transformations across untreated and treated paper samples. The dark regions in the SEM image of the untreated sample (Figure 6a) indicate areas rich in light elements, predominantly carbon and oxygen, typical of organic materials.

Notably, comparison with treated samples reveals significant differences, especially in those washed with distilled water (Figure 6b). In these samples, the residual additives and mineral fillers are effectively removed, resulting in clean cellulose fiber surfaces.

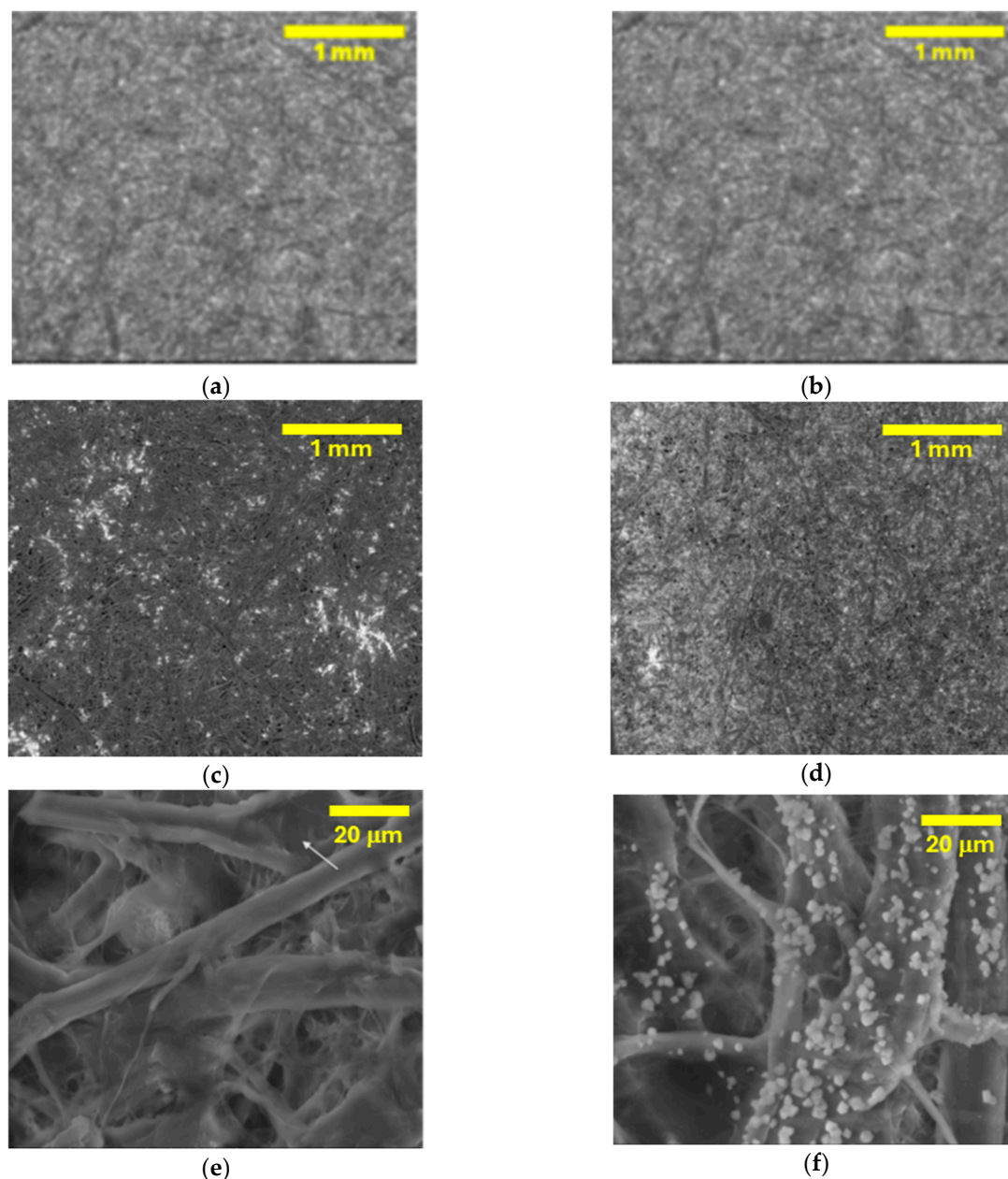


**Figure 6.** (a) SEM image of untreated sample A; on the right, image of the sample treated with distilled water (b). SEM images of samples treated with 5% concentration seawater dried at room temperature (c) and at  $T = 50\text{ }^{\circ}\text{C}$  (d). SEM images of azure paper samples subjected to treatment with 5% concentration seawater (e), sample dried at room temperature (f), sample dried at  $T = 50\text{ }^{\circ}\text{C}$ .

Elemental analysis further validates these findings, revealing the presence of silicon (Si), potassium (K), and aluminum (Al), indicative of mineral fillers such as Kalsilite ( $\text{KAlSiO}_4$ ) and Kaolinite ( $\text{Al}_2\text{Si}_2\text{O}_5(\text{OH})_4$ ) commonly used in paper manufacturing processes.

Furthermore, SEM images of samples treated with 5% concentration seawater solution and dried at different temperatures reveal variations in salt distribution patterns. While samples dried at room temperature (Figure 6c,e) exhibit salt aggregation in localized regions, attributed to the slower drying process allowing water accumulation and subsequent salt deposition, samples dried at  $50\text{ }^{\circ}\text{C}$  (Figure 6d,f) display a more uniform distribution of salts across the surface, indicative of rapid evaporation and homogeneous salt deposition.

These observations underscore the significant influence of drying conditions on salt distribution and deposition dynamics, with implications for the structural integrity and preservation of paper substrates.

Moreover, analysis through the kinetic model of paper reveals that treatments inducing variations exceeding an 8% error are considered significant, with the treatment involving seawater immersion and room temperature drying demonstrating the most pronounced effects. Interestingly, samples composed of pure cellulose exhibit minimal variations beyond the threshold of significance, suggesting inconsequential effects of treatments on these substrates.

For azure paper, primarily derived from cotton and linen rags, SEM images of samples treated with 5% concentration seawater and dried at 50 °C show a distinctive pattern of salt microcrystals covering around fibers rather than penetrating interstitial spaces. This phenomenon suggests that rapid drying impedes water accumulation, leading to the formation of salt clusters around fibers.

Notably, images of samples dried at room temperature further elucidate the influence of drying conditions on fiber integrity, with observations of fiber breakage potentially linked to salt-induced structural alterations. However, these hypotheses deserve further investigation through targeted and comprehensive studies to delineate the precise mechanisms underlying these observations.

#### 4. Conclusions

In this work, a preliminary study was conducted to examine the effects that may occur when paper is immersed in saline solutions of varying concentrations. Various types of paper were used, including modern Fabriano paper, “cinquecentine” paper, azure paper, and printing paper. Whatman 1 paper was used as the standard reference sample because it is composed of pure cellulose, the main component common to all types of paper.

Luminescence measurements underlined the different optical properties of the studied samples attributed to the different composition and possible presence of additives.

Raman spectroscopy was employed to study the trends of cellulose crystallinity index and polymerization degree concerning both drying temperature and the concentration and composition of the solution used. The analysis revealed that the most significant effects were observed for samples immersed in seawater solution and subjected to drying at  $T = 25\text{ °C}$  (slow drying).

Reflectance measurements highlighted that in samples containing additives, the reflectance curves show different trends for the UV and visible regions. Again, as observed in luminescence, variations between treated and untreated samples were noted, suggesting that treatments may eliminate bleaching agents or mineral charges used in paper production.

Thanks to reflectance measurements, a colorimetric study was conducted, with the most evident variations observed in sample C, the azure paper. The treatment that showed the greatest effects in this case was seawater at 1% concentration and drying process at  $T = 50\text{ °C}$ . The greatest variation in terms of colorimetric coordinates was manifested for coordinate *b*, showing that, following the treatment, the sample tends to shift its color from yellow towards blue, and thus appear whiter.

Finally, the images acquired with SEM have allowed highlighting the differences that may be present between samples treated with distilled water alone and with seawater at 5% concentration (i.e., the most extreme treatments) and dried either at room temperature or at  $T = 50\text{ °C}$ . It was observed that, with the same treatment using seawater at 5% concentration, the drying process can significantly influence the result. Slow drying might provide enough time for water to gather in specific areas, leaving concentrated salt deposits in these regions

once it evaporates. In the case of fast drying, this does not happen because salt crystals distribute uniformly over the entire sample and tend to adhere to the fibers.

EDX analysis confirmed the presence of elements attributable to additives such as Caolinite and Kalsilite, particularly highlighted in the azure paper.

This work aims to be the starting point for studying new techniques to study paper that have been immersed in saline solutions for some reason. Being a preliminary study, only effects for a limited number of concentrations were investigated; it would be advisable to increase this number for a more in-depth study.

To advance this research, next steps will focus on the study a wider range of saline concentrations and compositions, including synthetic seawater, and develop a mathematical model to predict the long-term interactions between salts and cellulose fibers, considering environmental factors like humidity and temperature. Further investigation will be focused into the distribution of salt deposits and their effects on fibers, using advanced imaging techniques. Expanding the study to include papers with inks and pigments will provide insights into their stability under saline treatments. Lastly, the dual role of salt as a mold inhibitor and potential preservative will be explored to assess its long-term impact on paper integrity.

**Supplementary Materials:** The following supporting information can be downloaded at: <https://www.mdpi.com/article/10.3390/heritage8020040/s1>, S1: Luminescence at 546 nm; S2: Variation of cristallinity index and polimerization degree of the studied samples; S3: Reflectance spectra; S4 Samples; Table S1: Summary of the studied samples.

**Author Contributions:** T.C.D.: Investigation, Formal analysis. F.A.P.: Investigation, Formal analysis. S.P.: Investigation, Formal analysis, Conceptualization, Writing—original draft, Validation, Writing—review and editing. C.M.C.: Writing—original draft, Validation. J.K.: Methodology, Investigation. D.C.: Writing—original draft, Validation, Methodology, Investigation, Formal analysis, Data curation, Conceptualization; Writing—review and editing, Supervision, Project administration, Methodology, Funding acquisition. All authors have read and agreed to the published version of the manuscript.

**Funding:** This research was funded by Fondazione di Sardegna, project FDS2022 “New diagnostic techniques for ancient books restauration and conservation” CUP F73C23001560007.

**Data Availability Statement:** Data will be made available on request.

**Acknowledgments:** The authors thank the Stare Archive of Cagliari for the support.

**Conflicts of Interest:** The authors declare no conflict of interest.

## References

1. Ministero per i Beni e le Attività Culturali Direzione Generale per gli Archivi. *Chimica e Biologia Applicate Alla Conservazione Degli Archivi*; Ministero per i Beni e le Attività Culturali Direzione Generale per gli Archivi, Direzione Generale per gli Archivi: Roma, Italy, 2002; Volume 74, ISBN 9788871252360.
2. Jablonsky, M.; Šima, J. Oxidative degradation of paper—A minireview. *J. Cult. Herit.* **2021**, *48*, 269–276. [[CrossRef](#)]
3. Nitiu, D.S.; Mallo, A.C.; Saparrat, M.C.N. Fungal melanins that deteriorate paper cultural heritage: An overview. *Mycologia* **2020**, *112*, 859–870. [[CrossRef](#)] [[PubMed](#)]
4. Goedvriend, G.J.M. Papermaking past and present. *Endeavour* **1988**, *12*, 38–43. [[CrossRef](#)]
5. Manso, M.; Costa, M.; Carvalho, M.L. Comparison of elemental content on modern and ancient papers by EDXRF. *Appl. Phys. A Mater. Sci. Process.* **2008**, *90*, 43–48. [[CrossRef](#)]
6. Jain, P.; Gupta, C. A sustainable journey of handmade paper from past to present: A review. *Probl. Ekorozwoju* **2021**, *16*, 234–244. [[CrossRef](#)]
7. Meusbürger, P. *Mobilities of Knowledge*; Springer International Publishing: Cham, Switzerland, 2017; ISBN 9783319446530.
8. Rusydiana, A.S. DigitalCommons @ University of Nebraska—Lincoln History of Libraries in the Islamic Period. 2021. Available online: <https://digitalcommons.unl.edu/libphilprac/6607/> (accessed on 6 January 2025).

9. Çiçekler, M.; Tutuş, A. Biodiversity and the Paper Industry: Forest Management and Nature Conservation. In Proceedings of the 4th International Conference on Innovative Academic Studies Biodiversity and the Paper Industry: Forest Management and Nature Conservation, Konya, Turkey, 12–13 March 2024.
10. Kolbe, G. Gelatine in Historical Paper Production and as Inhibiting Agent for Iron-Gall Ink Corrosion on Paper. *Restaur. Int. J. Preserv. Libr. Arch. Mater.* **2004**, *25*, 26–39. [[CrossRef](#)]
11. Florek, S. Copyright © 2020 seFlorek Copyright © 2020 seFlorek. 2020, 1–17.
12. Stephens, C.H.; Barrett, T.; Whitmore, P.M.; Wade, J.A.; Mazurek, J.; Schilling, M. Composition and Condition of Naturally Aged Papers. *J. Am. Inst. Conserv.* **2008**, *47*, 201–215. [[CrossRef](#)]
13. Novotny, M.; Laestadius, S. Beyond papermaking: Technology and market shifts for wood-based biomass industries—Management implications for large-scale industries. *Technol. Anal. Strateg. Manag.* **2014**, *26*, 875–891. [[CrossRef](#)]
14. Özden, Ö.; Sönmez, S.; Öztürk, A. Effect of Different Filler on Printability and Paper Properties. In Proceedings of the Innovations in Publishing, Printing and Multimedia Technologies 2020, Kaunas, Lithuania, 19–20 October 2020.
15. Becker, H. Growing and Hand Processing Fibre Flax and Hemp for Hand Papermaking. In Proceedings of the 2008 Int. Conf. Flax Other Bast Plants, Saskatoon, SK, Canada, 20–23 July 2008; pp. 150–158, ISBN 978-0-9809664-0-4.
16. Debnath, M.; Salem, K.S.; Naithani, V.; Musten, E.; Hubbe, M.A.; Pal, L. Soft mechanical treatments of recycled fibers using a high-shear homogenizer for tissue and hygiene products. *Cellulose* **2021**, *28*, 7981–7994. [[CrossRef](#)]
17. Beadle, C.; Stevens, H.P. Hand-made papers of different periods. *J. R. Soc. Arts* **1909**, *57*, 292–304.
18. Bhodiwal, S.; Chauhan, S.; Agarwal, R.; Barupal, T. A novel approach: Handmade papermaking. *MOJ Ecol. Environ. Sci.* **2022**, *7*, 11–16. [[CrossRef](#)]
19. Laurentius, F.; Laurentius, T. Chapter 1 The History of Paper in Europe. In *The History of Paper in Europe*; Brill: Leiden, The Netherlands, 2023; pp. 3–21. ISBN 9789004506848.
20. Mendoza, M.A.D.; De La Hoz Franco, E.; Gómez, J.E.G. Technologies for the Preservation of Cultural Heritage—A Systematic Review of the Literature. *Sustainability* **2023**, *15*, 1059. [[CrossRef](#)]
21. Giorgi, R.; Dei, L.; Ceccato, M.; Schettino, C.; Baglioni, P. Nanotechnologies for conservation of cultural heritage: Paper and canvas deacidification. *Langmuir* **2002**, *18*, 8198–8203. [[CrossRef](#)]
22. Odlyha, M. Introduction to the preservation of cultural heritage. *J. Therm. Anal. Calorim.* **2011**, *104*, 399–403. [[CrossRef](#)]
23. Area, M.C.; Cheradame, H. Paper aging and degradation: Recent findings and research methods. *BioResources* **2011**, *6*, 5307–5337. [[CrossRef](#)]
24. Alves, C.; Figueiredo, C.A.M.; Sanjurjo-Sánchez, J.; Hernández, A.C. Salt weathering of natural stone: A review of comparative laboratory studies. *Heritage* **2021**, *4*, 1554–1565. [[CrossRef](#)]
25. Higashijima, K.; Hori, C.; Igarashi, K.; Enomae, T.; Isogai, A. First aid for flood-damaged paper using saltwater: The inhibiting effect of saltwater on mold growth. *Stud. Conserv.* **2012**, *57*, 164–171. [[CrossRef](#)]
26. Bunyaphiphat, T.; Nakagawa-Izumi, A.; Enomae, T. Influences of saltwater immersion on properties of wood-cellulosic paper. *Carbohydr. Polym.* **2015**, *116*, 255–260. [[CrossRef](#)]
27. Millero, F.J.; Feistel, R.; Wright, D.G.; McDougall, T.J. The composition of Standard Seawater and the definition of the Reference-Composition Salinity Scale. *Deep Sea Res. Part I Oceanogr. Res. Pap.* **2008**, *55*, 50–72. [[CrossRef](#)]
28. Chiriu, D.; Pisu, F.A.; Ricci, P.C.; Carbonaro, C.M. Application of raman spectroscopy to ancient materials: Models and results from archaeometric analyses. *Materials* **2020**, *13*, 2456. [[CrossRef](#)]
29. Chiriu, D.; Ricci, P.C.; Cappellini, G.; Salis, M.; Loddo, G.; Carbonaro, C.M. Ageing of ancient paper: A kinetic model of cellulose degradation from Raman spectra. *J. Raman Spectrosc.* **2018**, *49*, 1802–1811. [[CrossRef](#)]
30. Zhu, Z.; Zeng, L.; Li, W.; Tian, D.; Xu, W. Enhancing Persistent Luminescence of Cellulose by Dehydration for Label-Free Time-Resolved Imaging. *ACS Sustain. Chem. Eng.* **2021**, *9*, 17420–17426. [[CrossRef](#)]
31. Tofail, S.A.M.; Koumoulos, E.P.; Bandyopadhyay, A.; Bose, S.; O'Donoghue, L.; Charitidis, C. Additive manufacturing: Scientific and technological challenges, market uptake and opportunities. *Mater. Today* **2018**, *21*, 22–37. [[CrossRef](#)]

**Disclaimer/Publisher's Note:** The statements, opinions and data contained in all publications are solely those of the individual author(s) and contributor(s) and not of MDPI and/or the editor(s). MDPI and/or the editor(s) disclaim responsibility for any injury to people or property resulting from any ideas, methods, instructions or products referred to in the content.